Environ. Sci. Technol. **2003**, *37,* 3555−3559

Fate of Uranyl in a Quaternary System Composed of Uranyl, Citrate, Goethite, and *Pseudomonas fluorescens*

RIZLAN BENCHEIKH-LATMANI,*,† JAMES O. LECKIE,† AND JOHN R. BARGAR‡

Department of Civil and Environmental Engineering and Stanford Synchrotron Radiation Laboratory, Stanford University, California 94305

This study investigated the partitioning of uranyl within a quaternary system made up of uranyl, citrate, goethite, and the bacterium *Pseudomonas fluorescens*. In the absence of cells, uranyl was sorbed to goethite as a complex involving surface groups and/or citrate. Measurements of the evolution of CO_2 indicated that the addition of bacterial cells lead to the gradual biodegradation of citrate. Throughout the biodegradation process, uranyl remained sorbed to the insoluble fraction comprised of goethite and cells. EXAFS (Extended X-ray Absorption Fine Structure) measurements showed that bacterial cells outcompeted goethite for uranyl under the experimental conditions and caused the repartitioning of uranyl from goethite to cell matter, independently from citrate degradation. Citrate degradation caused further release of uranyl from goethite surfaces, followed by subsequent association of uranyl with cells. At long equilibration times (3 months), cell lysis and phosphate release resulted in the precipitation of an autunite-like phase. This work suggests that bacterial degradation of uranyl-complexing ligands in contaminated subsurface media containing iron oxides should not necessarily lead to an increase in the mobility of uranyl.

Introduction

Iron oxides play an important role in immobilizing uranyl (UO_2^{2+}) in the subsurface through sorption. Furthermore, carboxylic acids that frequently co-occur with uranyl in contaminated DOE sites (*1*) can enhance uranyl sorption. Citrate, for example, is an excellent model for carboxylate complexing ligands and is a contaminant of concern due to its use as a complexing agent during radioactive materials and waste processing activities within the United States nuclear complex. Citrate has been shown to enhance the partitioning of uranyl onto goethite by up to 90% (depending upon chemical conditions) in the pH range 3−6 (*2*) by formation of a ternary surface complex involving citrate, goethite, and uranyl (*3*). The bacterially mediated degradation of citrate could reverse this enhancement, leading to the release of U(VI) bound to goethite. In addition, bacterial cells can directly sorb U(VI) and/or release phosphate, which may react with U(VI) to precipitate solid U(VI)-phosphate phases.

The goal of the present study is to investigate the partitioning of uranyl among phases in an oxygenated quaternary system that includes citrate, uranyl, goethite, and bacterial cells capable of degrading citrate (*Pseudomonas fluorescens*). *Pseudomonas fluorescens* is a common subsurface bacterium and therefore an appropriate model organism for this investigation. The main question this study aims to tackle is the fate of uranyl during citrate biodegradation.

This study builds on two prior studies of closely related ternary systems: an EXAFS structural characterization of uranyl surface complexes with goethite in the presence of citrate (*2*, *3*) and a detailed investigation of the inhibitory effect of uranyl on citrate biodegradation by *P. fluorescens* in the absence of a mineral phase (*4*). In the former, citrate was found to enhance sorption of uranyl onto goethite (*2*), and this effect was attributed to the presence of >Fe−L−U ternary complexes (i.e., ligand-bridging surface complex with goethite surface functional groups). In the latter, uranyl was found to inhibit the biodegradation of citrate by *P. fluorescens* by associating with the bacterial cell envelope (*4*): the greater the amount of uranyl sorbed per cell, the slower the rate of citrate biodegradation. These results suggest that if the amount of uranyl sorbed onto cells is low enough to permit bacterial degradation of citrate, then surface-bound uranyl (i.e., as >Fe−L−U complexes) may be released to solution. It follows that, at a contaminated field location, bacterial degradation of citrate could lead to an increase in uranium mobility. However, at least three processes could act to attenuate uranyl should it be released to groundwater from Fe oxide surfaces following citrate degradation: (a) uranyl could bind at the surfaces of cells, (b) uranyl could resorb onto a goethite surface modified by reaction with bacterial exopolymers, or (c) uranyl could precipitate as uranyl phosphate due to the release of phosphate from the bacteria. The previous investigations of the two above-mentioned ternary subsystems leave unresolved the ultimate fate of uranyl in the quaternary system. Therefore, direct measurement of uranyl species using techniques capable of quantifying the distribution of uranyl in the quaternary system are required.

Several previous studies have investigated the interaction of bacteria with uranyl in binary systems including sorption of uranyl to the surfaces of bacteria (*5*), the inhibition of bacterial metabolism by uranyl (*6*), and the secretion of phosphate by bacteria leading to the precipitation of uranyl phosphate (*7*). The present study is novel in that it investigates the fate of uranyl in a complex biogeochemical assemblage, a crucial step toward a more accurate representation of groundwater conditions at some DOE sites. It is the only study, to our knowledge, to investigate the fate of uranyl in a heterogeneous system where a complex geochemical system (citrate enhances uranyl sorption to goethite) and a biological interaction (*P. fluorescens* degrades citrate) are intertwined.

The majority of measurements presented herein were conducted at pH 5 for two reasons: (1) pH 5 is a reasonable pH for contaminated sites such as Savannah River and (2) low carbonate concentrations preclude the formation of U(VI)−carbonate complexes that would dominate the speciation at pHs > 6.5.

The present work shows that, in the presence of cells, uranyl initially sorbed onto goethite as a combination of >Fe−U and >Fe−L−U complexes, desorbed from goethite and sorbed onto cells as a result of two processes: (1) direct competition of cells for uranyl sorbed onto goethite as the >Fe−U complex and (2) citrate degradation, followed by the

* Corresponding author phone: (858)822-3140; e-mail: rizlan@ucsd.edu. Current address: Scripps Institution of Oceanography, Marine Biology Research Division, 9500 Gilman Drive, La Jolla, CA 92093-0202.

† Department of Civil and Environmental Engineering.

‡ Stanford Synchrotron Radiation Laboratory.

10.1021/es0210401 CCC: $25.00
Published on Web 07/09/2003

release of uranyl from the >Fe−L−U complex. Finally, cell lysis, which becomes significant after ~10 days of reaction, releases phosphate which precipitates with uranyl to form an autunite-like phase.

Experimental Section

Goethite Preparation. Goethite was prepared according to a modified version of the method of Atkinson et al. (*8*) under an Ar headspace and confirmed by X-ray Diffraction (XRD). The goethite was dialyzed in trace-metal-free dialysis tubing (Spectra Por 7, Spectrum Laboratories, New Brunswick, NJ) against deionized water and put through 10 centrifuge−decant−refill−agitate cycles to remove the very fine particle fraction and thus facilitate solid separation in subsequent experiments. The final surface area of the goethite was 90 $m^2.[g]^{-1}$ as determined by BET analysis (Coulter Surface Area Analyzer SA 3100).

Effect of Citrate on the Sorption of Uranyl on Goethite. Uranyl sorption onto goethite in the presence and absence of citrate was evaluated by measuring pH dependent sorption curves. Goethite (0.2 $g.[L]^{-1}$), suspended in buffer pH 5 (0.1 M KCl and 20 mM piperazine adjusted to pH 5.0), was autoclaved. KCl was present as a swamping electrolyte to control ionic strength, and piperazine is a buffer with a pK_a of 5.55. XRD analysis of the autoclaved solid indicated that no phase change resulted from autoclaving. Filter-sterilized citrate (sodium citrate dihydrate, Mallinckrodt, Phillipsburg, NJ) and uranyl (uranyl nitrate, Johnson Matthey, Ward Hill, MA) were added to the goethite suspensions in that order, to a final concentration of 1, 2, or 3 μM for citrate and 1 μM for uranyl. In some cases, citrate was added along with 10 μL of filter-sterilized [1,5]^{14}C-citrate (Sigma Chemical Co., St. Louis, MO; 4.16 $\mu Ci.[mL]^{-1}$). The pH was adjusted to 2.5 by adding HCl (J. T. Baker, Phillipsburg, NJ, Baker analyzed). The pH of the suspension was incrementally increased by addition of KOH (J. T. Baker, Phillipsburg, NJ, Baker analyzed). A subsample was collected aseptically at each 0.5 pH unit up to pH 7.5, placed in a sterile polycarbonate Oak Ridge tube, and allowed to equilibrate on an end-to-end shaker at 25 °C for 24 h. At that time, the pH in each tube was measured and taken to be the equilibrium pH, and the tubes were centrifuged at 1000*g* for 15 min. The supernatant was filtered with a 0.22 μm low-uranyl binding (<3% for 1 μM uranyl at pH 6.0) GVHP filter (Millipore Corporation, Bedford, MA) and analyzed by inductively coupled plasma mass spectrometry (ICP-MS HP 4500 series). Citrate sorption was quantified by liquid scintillation counting. All experiments were conducted in polycarbonate (PC) bottles to minimize sorption of uranyl and citrate to the container walls (<3% for both uranyl and citrate). Sorption experiments conducted with or without piperazine yielded identical results indicating no effect of piperazine on citrate or uranyl sorption.

Cell Growth Conditions. *Pseudomonas fluorescens* ATCC 55241 biovar II was kindly provided by A. J. Francis (Brookhaven National Laboratory, Upton, NY). Cells of *P. fluorescens* were grown at 25 °C in a sterile defined mineral salts growth medium dubbed MM2 and amended with filter-sterilized (Nalgene 0.2 μm PES syringe filter, Nalge Co., Rochester, NY) citric acid at a final concentration of 1 mM. One liter of MM2 contains 35.8 mg of NH_4Cl, 2.75 mg of $CaCl_2{\cdot}2H_2O$, 6.25 mg of $MgCl_2{\cdot}6H_2O$, 5.5 mg of KH_2PO_4, 2.585 mg $Fe(SO_4)_2NH_4{\cdot}12H_2O$, 1.155 mg of $MnSO_4{\cdot}H_2O$, 0.101 mg of $CuCl_2{\cdot}2H_2O$, 0.095 mg of $Na_2MoO_4{\cdot}2H_2O$, 0.165 mg of $ZnSO_4{\cdot}7H_2O$, 0.151 mg of $CoCl_2{\cdot}6H_2O$, 2.13 g of MES (2-(N-morpholino)ethanesulfonic acid, Sigma Chemical Co., St Louis, MO), 7.4 g of KCl (Sigma) and was adjusted to pH 6.0 ± 0.1. After 16−18 h (exponential phase), the cells were harvested by centrifugation at 10 800*g* for 30 min at 25 °C, washed twice with buffer pH 5, and concentrated in the same buffer (1 L of cells to 100 mL). This cell concentrate was used for all experiments.

Degradation of Sorbed Citrate and Fate of Uranyl. To evaluate the degradation of citrate sorbed to goethite and the fate of uranyl after citrate degradation, a series of batch experiments was conducted. A slurry of 0.2 $g.[L]^{-1}$ of goethite was prepared in buffer pH 5 buffer (see above). The slurry (25 mL) was placed in 500-mL PC bottles in 20 replicates and autoclaved. A mixture of unlabeled and [1,5]^{14}C-citrate was added to the goethite slurry in each bottle, followed by uranyl. The bottles were placed on a rotary shaker (100 rpm) at 25 °C for >4 h, a time which was determined to be sufficient to attain >99% uranyl sorption (for 1 μM uranyl) and 99% citrate sorption onto goethite. Cells were added to a final OD_{600} of 0.25. A base trap consisting of a scintillation vial containing 1 mL of 1 N KOH was suspended in the headspace of each bottle using Teflon tape. As citrate was degraded aerobically by *P. fluorescens*, ^{14}C-CO_2 was produced and trapped in the base trap; a mass balance of 95−102% was obtained for ^{14}C through desorption of ^{14}C-citrate at pH 13 for 14 h. At time intervals, duplicate bottles were sacrificed, and the amount of degraded citrate was measured by counting the ^{14}C content of the base trap. For the same sample, the slurry was filtered (0.22 micron GVHP filter), and the filtrate was analyzed for uranyl by ICP-MS and for Fe by Graphite Furnace Atomic Absorption (GFAA; Varian Spectra GTA 100). However, the background concentration of Fe (from piperazine) in the pH 5 buffer was sufficiently high (0.7 μM) to prevent meaningful quantification of solution Fe. pH remained at 5.0 ± 0.1 in all cases.

EXAFS. A goethite suspension in buffer pH 5 was prepared and sterilized by autoclaving. After cooling, the slurry was amended with citrate and uranyl (in that order) to reach the target concentration and allowed to equilibrate for 4−8 h. An appropriate volume of a stock of *P. fluorescens* cells was added to the slurry to obtain the desired equivalent OD_{600}. The uranyl concentration was increased as compared to that used for non-EXAFS experiments to address limitations in the sensitivity of EXAFS. Consequently, the concentrations of citrate (75 μM) and goethite (1 $g.[L]^{-1}$) were also raised (relative to the non-EXAFS experiments) to ensure that uranyl was sorbed <80% without citrate and ≥95% with citrate. A parallel experiment was conducted with ^{14}C citrate to quantify citrate degradation using a base trap as described above.

After the prescribed equilibration time, the samples were centrifuged at 10 800*g* for 30 min. The resulting paste was transferred to 2-mm Teflon sample holders with polycarbonate windows and stored at 4 °C. EXAFS analysis of the samples began no longer than 12 h after sample preparation. For the uranyl sorbed onto cells, uranyl was added to freshly harvested vegetative cells at the adequate concentration suspended in buffer pH 5. The samples were allowed to equilibrate for a maximum of 4 h to minimize cell lysis and precipitation of a uranyl-phosphate phase. Uranium L-III edge EXAFS spectra were collected at room temperature at the Stanford Synchrotron Radiation Laboratory beamline 4-3 as described elsewhere (*3*) and were processed using the software package EXAFSPAK (*9*). Absorption spectra were background-subtracted, spline-fitted, and k^3-weighted to obtain the EXAFS spectra.

The EXAFS spectra were fitted (using the program DATFIT included in EXAFSPAK) with linear combinations (LC) of spectra from the four components known to be present in this system based on previous work and/or present knowledge. These include two distinct uranyl−goethite surface complexes (i.e., a binary goethite−uranyl complex, designated >Fe−U, and a ternary >Fe−citrate−U complex) (*3*), cell-sorbed uranyl, and autunite ($Ca(UO_2)_2(PO_4)_2{\cdot}10H_2O$) (*10*). Each component and sample spectrum was isolated using splines having 3, 4, and 5 ranges in order to evaluate the extent of low frequency amplitude introduced into the EXAFS

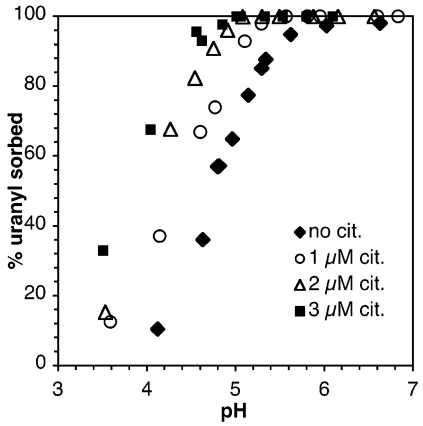

FIGURE 1. Uranyl sorption onto goethite (0.2 g/L) in the presence of 0.1 M KCl and 20 mM piperazine. Citrate concentrations: none (diamonds), 1 μM (circles), 2 μM (triangles), and 3 μM (squares).

by the spline function. In general, spline-related amplitude was found to cause the fit residual to vary by up to approximately a factor of 5, corresponding to differences in fit-determined values of several percent. The spline providing the lowest residual (during LC fitting) was retained. This procedure was tested by fitting spectra from physical mixtures of known amounts of autunite (which has an indistinguishable spectrum from chernikovite) and schoepite. The resulting calibration curve was found to have a slope of 1.0, and the average 1-sigma uncertainty was 6%, which derives primarily from low-frequency low-amplitude structure originating in the spline fit. Accordingly, we take 6% as an estimated 1-sigma for our linear combination fits.

Release of Phosphate. Freshly grown cells were washed and resuspended in pH 5 buffer in separate PC bottles. Uranyl was added to duplicate bottles, whereas another set of duplicates was left untouched. The bottles were shaken at 25 °C in the dark. At time intervals, each bottle was sampled, and the samples were filtered and analyzed for uranyl (by ICP-MS) and organic phosphate. Organic phosphate was analyzed by digestion with persulfate followed by colorimetric determination with ascorbic acid and ammonium molybdate (*11, 12*).

Results and Discussion

Citrate substantially enhanced uranyl sorption onto goethite from pH 3 to 6 (Figure 1). The maximum pH for which citrate enhanced uranyl sorption was greater in the present study than observed by Redden et al. (*2*) because the present study uses a lower total goethite surface area per volume ratio (18 $m^2.[L]^{-1}$) than Redden et al. (68 $m^2.[L]^{-1}$). Uranyl sorption on goethite was measured in the presence of CO_2. Carbonate has previously been shown to not affect uranyl sorption in this system at pH <6.5 (*13*). The question of interest is whether uranyl initially sorbed onto goethite in the presence of citrate is redistributed in the quarternary system (the additional component is bacteria) as a result of sorption onto cells and ongoing citrate biodegradation.

The degradation of citrate by *P. fluorescens* and the solution concentration of uranyl were monitored simultaneously (Figure 2). Prior to cell addition, 99% of uranyl was sorbed to goethite (in the presence of citrate), leaving 10 nM uranyl in solution. After cell addition, the solution uranyl concentration dropped below the detection limit of 5 nM for the remainder of the experiment (Figure 2): as citrate was degraded, uranyl did not reappear into solution. This result suggests sorption to cells occurred. It is in contrast to the effect of the degradation by *Chelatobacter heintzii* of NTA bound as an NTA−Co complex onto gibbsite. In that case, Co^{2+} accumulates in solution (*14*). The difference may be due to the lack of sorption of Co^{2+} to cell surfaces in contrast to uranyl that sorbs readily onto cells (*5*).

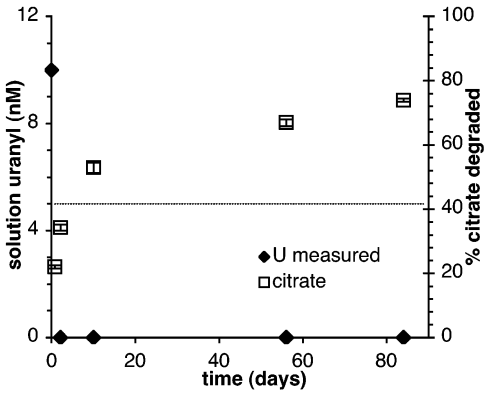

FIGURE 2. Uranyl solution concentration during citrate degradation. Citrate (2 μM), uranyl (1 μM) are initially sorbed ($t = 0$) on goethite (0.2 g.$[L]^{-1}$). Citrate degradation by *P. fluorescens* (OD_{600} 0.25) is depicted by squares. The measured solution uranyl concentration is largely below the detection limit of 5 nM (diamond) immediately after cell addition ($t = 0.5$ h).

TABLE 1. Summary of Conditions for EXAFS Samples

pH	goethite concn (g/L)	citrate concn (μM)	U concn (μM)	% U sorbed	OD_{600}	% citrate degraded	eq. time w/ cells
5	1	75	75	95			
5	1		75	76			
5	1	40	75	90			
5	1	75	75	95	0.5	1	4 h
5	1	75	75	95	0.5	45	9 days
5	1	75	75	95	0.5	72.5	3 months

TABLE 2. Summary of the Fits with EXAFSPAK[a]

	components			
equilibration time	U+cells	>Fe−U	>Fe−L−U	autunite
before cell addition	0	51	49	0
4 h	43	13	38	6
9 days	53	1	32	14
3 months	12			88

We used EXAFS as an independent method to probe directly the fate of uranyl in this quaternary system. Three identical samples containing uranyl, citrate, goethite, and *P. fluorescens* were allowed to equilibrate for 4 h, 9 days, and 3 months, respectively. The conditions for each sample are summarized in Table 1. In our previous EXAFS work (*3*), we have studied the ternary system uranyl, citrate, and goethite. Here we have extended that work by adding a fourth component: bacterial cells. Doing so required measurement of EXAFS spectra for two additional species, uranyl sorbed to *P. fluorescens* cells at pH 5 and that of autunite (a uranyl-phosphate phase) from Fuller et al. (*10*).

Prior to the addition of cells to the uranyl, citrate, goethite mixture, two surface uranyl complexes dominate uranyl speciation (*3*), namely uranyl directly bound to the goethite surface (>Fe−U) and uranyl bridged to the goethite surface through citrate (>Fe−L−U) (Table 2).

EXAFS spectra (Figure 3) for the uranyl−citrate−cell−goethite sample equilibrated 4 h were fitted with a combination of 43% of a spectrum of cell-bound uranyl, 38% of the goethite−citrate−complex, and 13% of the goethite−U complex (Table 2). Initially, before cell addition, 95% of uranyl was associated with goethite either directly (goethite−U complex) or indirectly (goethite−citrate−U complex) and

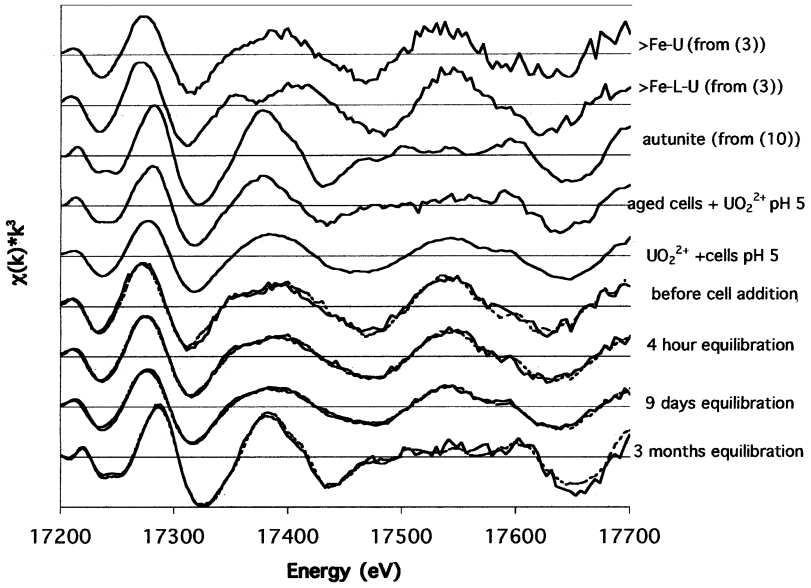

FIGURE 3. EXAFS data for components and linear combination fits of EXAFS data. Dotted lines are the fits. >Fe−U corresponds to a sample at pH 5.5 in the absence of citrate. >Fe−L−U corresponds to a sample at pH 3.5 in the presence of citrate. No uranyl sorption occurs at pH 3.5 in the absence of citrate (under these conditions) and thus sorption occurring in the presence of citrate is mediated by citrate.

5% was in solution. Therefore, uranyl associated with cells increased from 5% (assuming all the free uranyl sorbed to cells immediately upon their addition) to 43% after 4 h. Interestingly, the fraction of uranyl that remained sorbed to goethite after 4 h was dominated by the citrate-bridged (>Fe−L−U) complex. Additionally, the binary complex (>Fe−U) was consumed during the reaction suggesting it is not as stable as the former. Fits to the 4-h spectrum were attempted including autunite as a component and yielded a percent contribution at or below the detection limit (~6%).

Linear combination fits to the sample equilibrated for 9-days show that the majority (53%) of uranyl was associated with cells. The remainder of the fit was provided by the goethite−citrate−U (>Fe−L−U) complex (32%) and autunite (14%). The redistribution of uranyl from goethite to cell surfaces cannot be explained solely by the release of uranyl through the ongoing citrate degradation. After 9 days, 40 μM of citrate remain. A separate sorption experiment revealed that at pH 5, 90% of 75 μM of uranyl is sorbed onto 1 g.$[L]^{-1}$ goethite in the presence of 40 μM citrate (Table 1). This means that the biodegradation of 35 μM of citrate should release only 5% of the total uranyl (~4 μM), whereas 21% of uranyl was removed from the goethite surface. Therefore, redistribution of U from goethite to cells must be driven by uranyl sorption to cells and possibly precipitation of autunite.

The spectrum of the sample that was equilibrated for 3 months was best fitted by a combination of the spectrum of autunite (88%) and uranyl sorbed onto cells (12%). Neither of the goethite sorbed species contributed significantly to uranyl speciation. Citrate concentration after 3 months was 20 μM.

Mechanism of Uranyl Repartitioning. From the observations above it can be inferred that there are at least two processes by which uranyl is released from the goethite surface: (1) Cells bind U(VI), depleting its total concentration in aqueous solution (solute-phase uranyl is likely dominated by UO_2Cit^- (aq), which is the most abundant uranyl−citrate complex at low U(VI) and citrate concentrations) and leading to the mass-action release of uranyl complexed at goethite surfaces, even in the presence of citrate. It is also possible, although not required, that bacterial cells scavenge uranyl following direct contact with goethite. (2) Biodegradation of citrate depletes its total concentration in aqueous solution, leading to the mass-action release of citrate from goethite

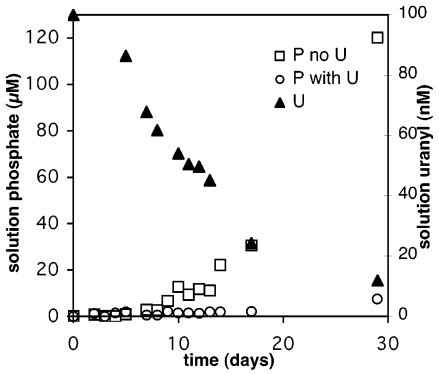

FIGURE 4. Solution phosphate from vegetative cells (OD_{600} 0.1) in buffer pH 5 in the presence of 1 μM uranyl (circles) or in the absence of uranyl (squares). Phosphate accumulates in solution in the absence of uranyl but not in the presence of uranyl due to the formation of an insoluble uranyl phosphate phase. Uranyl in solution (triangles). Cells are added at $t = 0$ and after 1 day, solution uranyl is 100 nM due to sorption to cells.

surfaces, with an attendant decrease in the sorptive capacity of goethite for uranyl. There is no net accumulation of uranyl in solution, suggesting that it rapidly sorbs onto the surfaces of *P. fluorescens*.

Role of Orthophosphate Released from Cell Lysis. Figure 4 shows that vegetative cells placed in a nongrowth buffer release phosphate into solution. After 29 days, phosphate builds up to approximately 120 μM in the absence of uranyl. The release of phosphate is due to aging and subsequent lysis of cells. In contrast, in the presence of uranyl, little phosphate accumulation is observed. This can be explained by the precipitation of a uranyl phosphate, autunite-like phase. Figure 3 shows that an EXAFS spectrum of cells aged with uranyl in a nongrowth buffer is similar to a spectrum for autunite. Surprisingly, the ratio of phosphate released relative to uranyl precipitated is large (>1000). This is likely due to the release of large organic, phosphate-rich molecules in which the majority of phosphato moieties are unavailable to bind uranyl. Upon digestion of the organic phosphate (as part of the analytical protocol), a large number of orthophosphate molecules are released, building up to a high concentration.

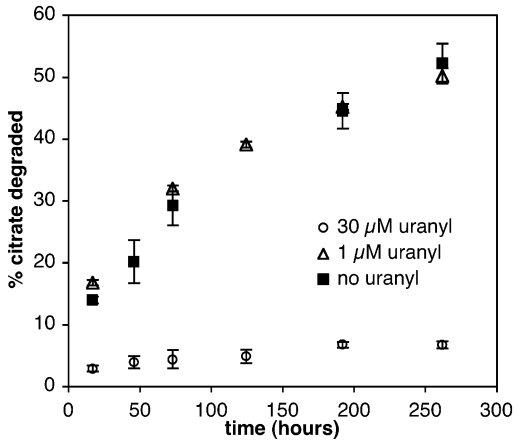

FIGURE 5. Effect of uranyl on the biodegradation of citrate (2 μM) initially sorbed onto goethite (0.2 g.[L]$^{-1}$) by *P. fluorescens* cells at OD_{600} 0.25 at pH 5. circles (30 μM uranyl), triangles (1 μM uranyl), and squares (no uranyl). Error bars corresponding to the range of the duplicates.

It appears as though, in the nutrient-poor environment mimicked in our experiment, the cells initially degrade citrate but eventually die and lyse, releasing phosphate, which, in turn, precipitates uranyl. The immobilization of uranyl in an insoluble uranyl phosphate phase is a highly desirable effect that reduces the bioavailability of uranyl.

The above phenomenon is distinct from the detoxification mechanism identified for *Citrobacter* sp. (*7*) whereby the cells excrete phosphate to precipitate metals as phosphate solids. In the case of UO_2^{2+} and *P. fluorescens*, the phosphate is released in the presence and absence of the radionuclide.

Summary and Environmental Relevance. The fate of uranyl is greatly affected by the presence of bacterial cells in a quaternary system. *P. fluorescens* cells bind uranyl regardless of whether citrate is degraded. We would expect the same result to happen at higher uranyl concentrations where the presence of uranyl inhibits citrate biodegradation (Figure 5). Cell death and lysis releases phosphate, which precipitates with uranyl as autunite.

Based on these results, it can be predicted that sites heavily contaminated with citrate and uranyl would not necessarily show citrate degradation, due to the inhibitory effect of uranyl on cell metabolism (Figure 5). Nevertheless uranyl attenuation could be enhanced by the presence of bacterial cells because of their high affinity for uranyl. Thus, even in the absence of citrate degradation, uranyl would be expected to associate preferentially with cell surfaces as a result of sorption competition. Because of the strong association of uranyl with cells, the colloidal transport of uranyl by cells may be an important mechanism and merits significant attention. Lysis of bacterial cells may contribute to the immobilization of uranyl by the release of phosphate and the precipitation of insoluble U-phosphate phases. Hence, citrate degradation in a citrate- and uranyl-contaminated site should not necessarily lead to an increase in the mobility of uranyl.

Acknowledgments

This work was supported by a grant from the Environmental Management Science Program in the Department of Energy (DE-FG07-96ER14698). Portions of this research were carried out at the Stanford Synchrotron Radiation Laboratory, a national user facility operated by Stanford University on behalf of the U.S. Department of Energy, Office of Basic Energy Sciences. We thank Dorothy Parker, Sandy Robertson, and Sam Webb for their careful review of the manuscript as well as abundant and useful comments.

Literature Cited

(1) Riley, R. G.; Zachara, J. M.; Wobber, F. J. U.S. DOE, 1992.
(2) Redden, G. D.; Li, J.; Leckie, J. O. In *Adsorption of Metals by Geomedia*; Jenne, E. A., Ed.; Academic Press: 1998.
(3) Redden, G. D.; Bargar, J.; Bencheikh-Latmani, R. *J. Colloid Interface Sci.* **2001**, *244*, 211−219.
(4) Bencheikh-Latmani, R.; Leckie, J. O. Accepted for publication in *Geochim. Cosmochim. Acta* **2003**.
(5) Haas, J. R.; DiChristina, T. J.; Wade, R., Jr. *Chem. Geol.* **2001**, *180*, 33−54.
(6) Tuoniven, O. H.; Kelly, D. P. *Arch. Microbiol.* **1974**, *95*, 153−164.
(7) Macaskie, L. E.; Empson, R. M.; Lin, F.; Tolley, M. R. *J. Chem. Technol. Biotechnol.* **1995**, *63*(1), 1−16.
(8) Atkinson, R. J.; Posner, A. M.; Quirk, J. P. *J. Phys. Chem.* **1967**, *71*(3) 550−558.
(9) George, G. N. EXAFSPAK, Stanford Synchrotron Radiation Laboratory, 1993.
(10) Fuller, C. C.; Bargar, J. R.; Davis, J. A.; Piana, M. J. *Environ. Sci. Technol.* **2002**, *36*(2), 158−165.
(11) Ames, B. N. In *Methods in Enzymology*; Colowick, S. P., Kaplan, N. O., Eds.; Academic Press: Orlando, 1996; Vol. 8, pp 115−118.
(12) AWWA. *Standard Methods for the Examination of Water and Wastewater*; 1998.
(13) Kohler, M.; Honeyman, B. D.; Leckie, J. O. Stanford University, 1994.
(14) Bolton, H.; Girvin, D. C. *Environ. Sci. Technol.* **1996**, *30*(6), 2057−2065.
(15) [a]The uncertainty in linear combination fits is 6%.

Received for review November 25, 2002. Revised manuscript received May 19, 2003. Accepted May 20, 2003.

ES0210401